RELATIONSHIP BETWEEN MICROSTRUCTURE AND FATIGUE DAMAGE OF ALTERNATOR FANS

Floriane Léaux[a], Jérémie Bouquerel[a], Jean-Bernard Vogt[a] and Frédéric Palleschi[b]

[a] UMET – UMR ENSCL/USTL/CNRS 8207, team Métallurgie Physique et Génie des Matériaux
Université Lille1, Bâtiment C6, 59655 Villeneuve d'Ascq, France
[b] VALEO Systèmes Electriques, 2, rue André Boulle, 94046 Créteil

Abstract. New car alternators cooled by fans are subjected to start-stop cycles, which cause fatigue damage and finally fracture. The complex shape of fans and the fatigue behaviour make life time predictions difficult. In this study, a damage criterion method is developed with a metallurgical approach. On one hand, fatigue specimens are subjected to various fatigue test conditions and the microstructural evolutions resulting from the cyclic plasticity are studied with a multi-scale metallurgical investigation. On the other hand, fans, unused and cycled on test bench, also undergo microstructural analysis. Comparing the results, fatigue damage criteria are proposed. These latter will be implemented in future for life time prediction of complex geometry fans.

1 CONTEXT OF THE PROJECT AND ISSUE

Because the design of new car alternator cooling fans must meet requirements, such as heat evacuation, weight reduction, noise-reducing and the function of start and stop, it results in a specific shape as shown Figure 1. In the present case, the damaging cyclic loading induces the failure of the fans by fatigue damage. Some parts contain slots which act as stress concentrator. Thus, even if the major part of the fan is elastically loaded, yielding can occur in the slot vicinity. Finite Element Method (FEM) has been used to determine the strain and stress levels and their location. Analyses were performed with the ANSYS finite element program. Figure 1 suggests that the material ahead slots at blades n°1 and n°6 of the fan are the most highly stressed. This has been confirmed by tests benches, which show that critical failures occur at these locations.

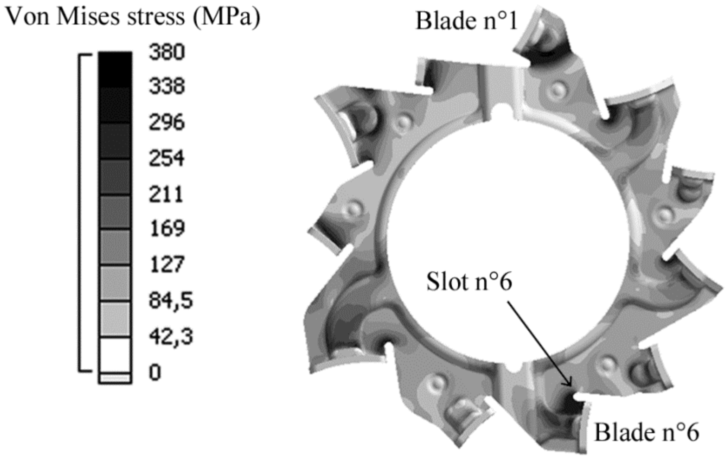

Figure 1 –Von Mises equivalent stress calculation showing critical locations of blades n°1 and n°6.

The main objective of this study consists in assessing the life time of the component in real conditions of use. For that, it is necessary to have a better understanding of the fatigue damage phenomenon combined with FEM calculations. The complex geometry will be taken into account as well as the fatigue behaviour of the material.

2 APPROACH OF THE PROJECT

Complementary techniques are considered to achieve this goal: FEM, fatigue study and metallurgical investigation. The great development of FEM calculations since the 1980s allows calculations of structures even more complex [1], [2]. By transforming load into local stress, FEM takes into account the effect of the geometry of the component (stress concentration). To obtain local strain, the method uses stress-strain equation which has to be representative of the mechanical material properties of the material. It is now widely accepted that data extracted from monotonic tensile test are not suitable to predict accurately the fatigue behaviour. Thus, FEM approach usually includes fatigue parameters from cyclic stress-strain curves and fatigue resistance curve. In our

study, appropriate fatigue tests under different strain loading signals will lead to find damaging conditions. Finally, an appropriate Low Cycle Fatigue (LCF) damage parameter based on metallurgical investigation will be proposed.
Previous studies predict fatigue life using FEM and fatigue parameters, such as cyclic stress relaxation [3]. If the component geometry is simple enough to use strain gages, then the experimental strain is directly measured on the component and compared with the strain calculated with FEM analysis [4]. In case of more complex shapes, measuring the local strain is a real problem especially in stress concentration areas. In case of elastic state or elastic state with small area of plasticity within large zones of elasticity, Neuber or FEM methods are applied with goods correlation with experimental results [5]. But in case of large plasticity (LCF for example), changes of microstructure might occur and influence the fatigue behaviour. In case of the alternator fans, strain is difficult to be measured (because of the complex shape) and to calculate (because of plastic strain), thus a metallurgical study of the material is necessary.
With this aim, a metallurgical investigation combining Transmission Electron Microscopy (TEM) and Electron Back Scattered Diffraction (EBSD) is developed in our study. Indeed, the development of dislocations structures, discernible by TEM, reflects the accommodation of the cyclic plasticity [6]. Nevertheless, since the so-found TEM observations concern in general a limited number of grains, quantitative method is needed to complete the metallurgical study. The EBSD method, frequently employed for phase identification [7-9] is nowadays widely used to determine local strain [10-12], grain size, texture analysis [9], [13], plastic strain assessment [14], ridging and rolling effects [15]... and becomes interesting for study of cyclic plasticity. Nevertheless, as yet, the EBSD technique has been rarely used for assessment of cyclic plasticity [16-18]. Yet, the use of different criteria based on misorientation distribution approaches leads to a correct evaluation of the local plastic strain at a mesoscopic scale. In addition, this method can be applied at any place of a part (e.g. in the root of a notch) and is able to make allowance for stress concentration effect of a notch. The microstructure changes are cyclic plasticity accommodation markers and are connected to the cyclic solicitation during fatigue life of lab specimens or of fans after real use. These understanding and quantifications allow to establish a damage criterion and a life time model based on the fatigue characteristics of the material. In our study, local strain in the lab specimens and in real fans broken in real conditions of use will be quantified and compared.

3 MATERIALS

An industrial steel provided by POSCO Company has been used in this study. Two batches were used, called SPCC and SPCD according to JIS G3141 norm. The very close chemical composition of both steels is given in Table 1.

Table 1 - Chemical composition of SPCC and SPCD steels.

(wt. %)	Fe	C	Si	Mn	P	S
SPCC	Bal.	0.0346	0.002	0.228	0.0063	0.0041
SPCD	Bal.	0.0437	0.005	0.247	0.0079	0.0066

Both steels also exhibit a ferritic equiaxed microstructure with a grain size of 11µm and a hardness of 112HV.

Table 2 gives the monotonic mechanical properties of the studied materials.

Table 2 - Mechanical properties of the tested materials.

	Young modulus GPa	0.2% yield strength MPa	Ultimate tensile strength (UTS) MPa	Uniform elongation %
SPCC	212	244	252	27
SPCD	210	260	259	27

Since the properties of both steels do not differ in term of microstructure and of mechanical behaviour, the different results for SPCC and SPCD will not be separated.

4 FATIGUE BEHAVIOUR

The fatigue tests are carried out using a MTS hydraulic machine with a load capacity of 2.5kN under a total fully reversed controlled strain (R_ε=-1). In all cases, the strain variation was kept constant ($\Delta\varepsilon_t$=0.3%, 0.4%, 0.5%, 0.7% or 1.0%). The tests were performed at room temperature with a triangular wave form at a strain rate of $1\times10^{-2}s^{-1}$. The fatigue specimens are plate with a thickness of 1.2mm, a width of 8mm and a gauge length of 15mm. The fatigue life is defined as the number of cycles leading to a drop of 25% of the tensile stress or leading to the fracture. Mid-life pseudo stabilised hysteresis loop is taking as a cycle reference.
The evolution of peak stress versus the number of cycles N in a logarithmic scale and versus the fatigue life fraction in a linear scale are reported in Figure 2(a) and Figure 2(b) respectively.

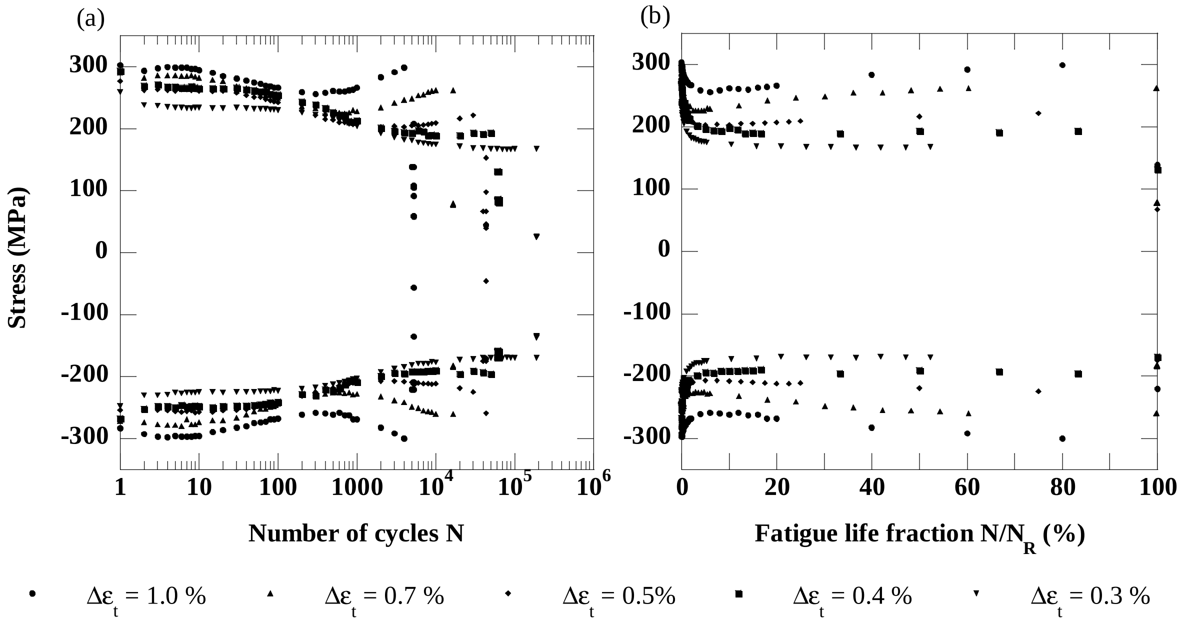

Figure 2 - Cyclic stress response as a function of the number of cycles N (a) and of the life fraction (b) for various strain range tests $\Delta\varepsilon_t$.

Under imposed strain, the response is characterised by a cyclic softening behaviour followed by a hardening period later in the fatigue life. The transition cycle between these two regimes decreases with the applied strain amplitude. For $\Delta\varepsilon_t$=1.0%, 0.7% and 0.5%, the hardening is clearly visible, whereas for $\Delta\varepsilon_t$=0.3% and 0.4%, the softening/hardening transition is not reached and the major life time consists of a slight softening.

From the pseudo stabilised loop, strain and stress amplitude values can be measured for the construction of the cyclic strain stress curve (CSSC) and of the strain fatigue resistance curve shown respectively in Figure 3(a) and Figure 3(b). It can be seen that the cyclic softening is all the more important that the strain range is low and tends to disappear at the highest strain range. In FEM calculations, the CSSC will be used instead of the monotonic curve.

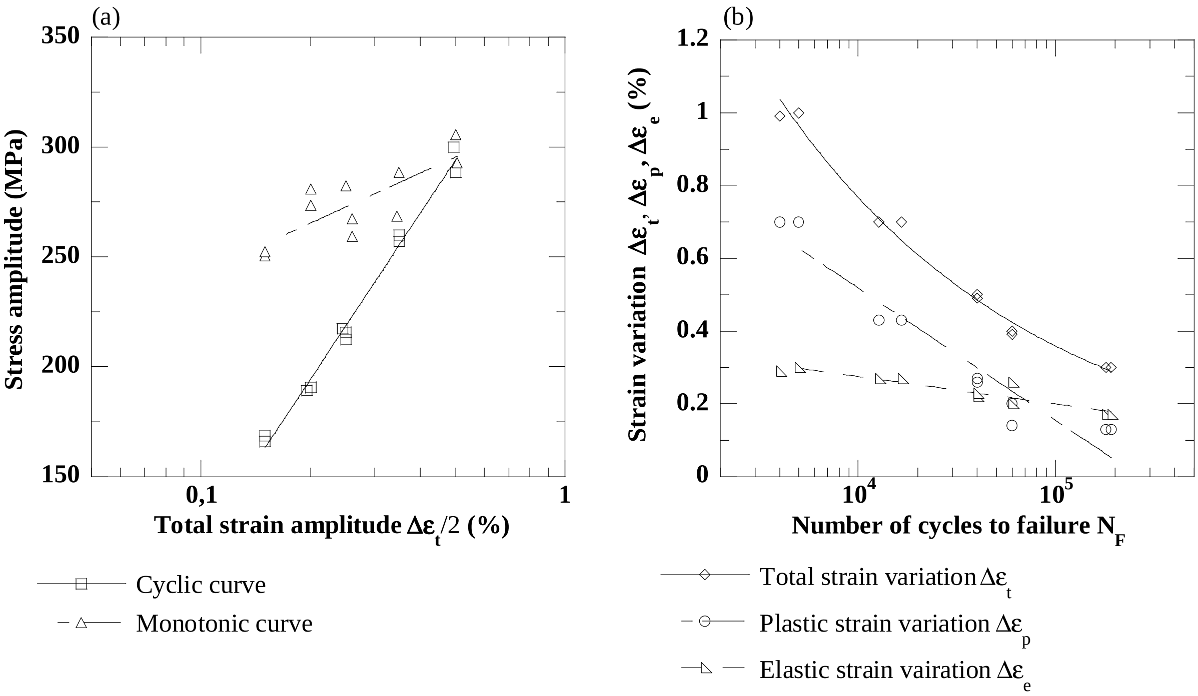

Figure 3 – Cyclic and monotonic strain stress curves (a) and fatigue life as a function of elastic, plastic and total strain range (b).

5 METALLURGICAL INVESTIGATIONS – ASSESSEMENT OF LOCAL PLASTICITY

5.1 Experimental procedure

5.1.1 Transmission Electronic Microscopy (TEM)

TEM investigations aimed at identification of the dislocations structures formed by cyclic plasticity. Fatigued specimens were cut using a low speed diamond saw. Samples were ground into 110µm thick slices using abrasive paper and punched into discs 3mm diameter. The discs were twin-jet polished using a solution of 95% acetic acid and 5% perchloric acid at 32V and 20°C. For microstructure observations, a FEI Technai G2 20 TEM under bright-field imaging (BFI) mode was used to obtain images.

5.1.2 Electron Backscattered Diffraction analysis (EBSD)

EBSD is employed to localise and estimate the local plastic strain for the fatigue specimens and alternator fans. The longitudinal section of an uncracked portion of the lab specimen was gently cut and the mid-plane was mechanically polished down to 0.25µm diamond, following by a final polishing using 0.02µm colloidal silica solution. Afterwards, the samples were examined in a FEI Quanta 400 SEM fitted with a HKL / Oxford Instruments EBSD system. Spatial resolution depends on microscope parameters [19] such as step size and spot size. The best step size is the largest step size such as misorientation distribution does not change [20]. Following these conditions, maps were obtained by scanning a selected area of the specimen, which is tilted 70° from the horizontal, at 20kV, with an optimal step size of 0.2µm and a spot size from 400nm to 550nm. Post treatment was made with HKL Channel 5 ®.

5.2 Results

5.2.1 TEM observations

The TEM micrographs of the reference specimen ($\Delta\varepsilon_t$=0% - unfatigued), as well as, the deformed samples ($\Delta\varepsilon_t$=0.5%) are shown in Figure 4.

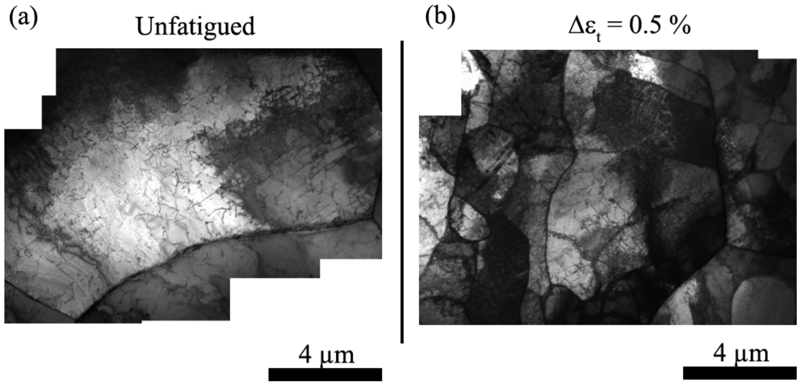

Figure 4 – TEM micrograph of the unfatigued specimen (a) and $\Delta\varepsilon_t$=0.5% fatigued specimen (b).

Unfatigued specimen exhibits a low but appreciable density of dislocations. These are homogenously distributed and probably results from the process. At the opposite, after fatigue at $\Delta\varepsilon_t$=0.5%, specimen has a high density of dislocations arranged in cells, characteristic of a strained low carbon ferritic steels [6], [21]. Within the cells the density of dislocations is also high. Specimens cycled at $\Delta\varepsilon_t$=0.7% also present cell dislocations structure with much smaller cell size. Thus, in the range of deformations studied, no other kind of dislocations arrangements (persistent slip band, labyrinth, dipolar wall) has been observed.

5.2.2 EBSD

Based on misorientation measurements, two approaches are considered to investigate the microstructure evolution: the Grain Boundaries (GB) study and the Kernel Average Misorientation (KAM).

- Grain boundaries characterisation: LAGB/HAGB measurements

Grain boundaries can be divided into two groups: the High Angle Grain Boundaries (HAGB) and the Low Angle Grain Boundaries (LAGB). LAGB are made of individual periodic defects. It results a misorientation up to 15°. When the core of the dislocations overlap, then the defects become continuous and the misorientation between the neighbouring grains is in excess of 15°. In that case, it consists of High Angle Grain Boundaries (HAGB).

When a material undergoes strain, dislocations arrangements develop. Dislocations walls or subgrains can be up to 10-15° misorientated. Studying these misorientations contributes to understand how the material accommodates an imposed plastic strain.

The GB maps of the reference specimen ($\Delta\varepsilon_t$=0% - unfatigued), as well as, the cycled samples ($\Delta\varepsilon_t$=0.3%, $\Delta\varepsilon_t$=0.5% and $\Delta\varepsilon_t$=0.7%) are shown in Figure 5. The reference specimen, as well as the lowest deformed sample ($\Delta\varepsilon_t$=0.3%) mainly exhibit misorientation angle over 15° which correspond to HAGB. For higher cyclic strain tests ($\Delta\varepsilon_t$=0.5% and $\Delta\varepsilon_t$=0.7%), in addition to HAGB, the GB maps comprise the LAGB. Besides, some grains appear as free of LAGB whereas other grains exhibit a high LAGB density, which suggest a heterogeneous partition of the deformation. Dislocations cell structures form preferentially on the most plastically deformed grains which are the best oriented ones for the plastic deformation and which are all more numerous than the applied strain is high. These results, quantified in Figure 6, could be separated into two groups: first, $\Delta\varepsilon_t$=0.5% and 0.7% present a high amount of LAGB, whereas reference specimen and $\Delta\varepsilon_t$=0.3%, show very small LAGB fraction values.

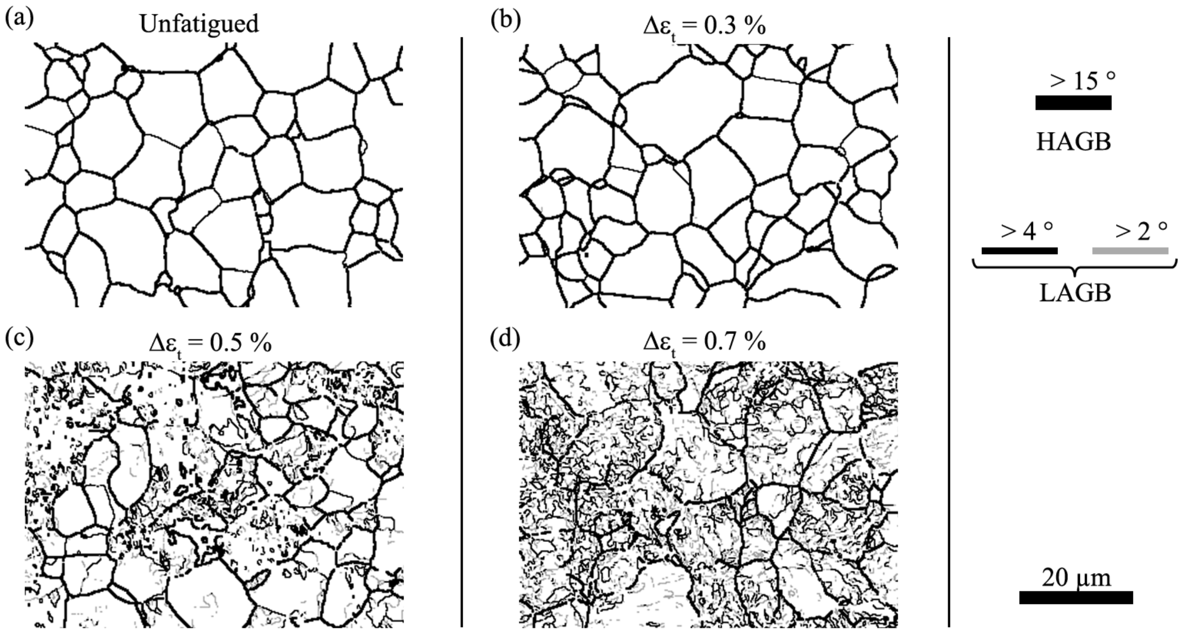

Figure 5 – GB map for the unfatigued specimen ($\Delta\varepsilon_t$=0%) (a), the $\Delta\varepsilon_t$= 0.3% fatigued specimen, (b), $\Delta\varepsilon_t$= 0.5% fatigued specimen (c) and the $\Delta\varepsilon_t$=0.7% fatigued specimen (d).

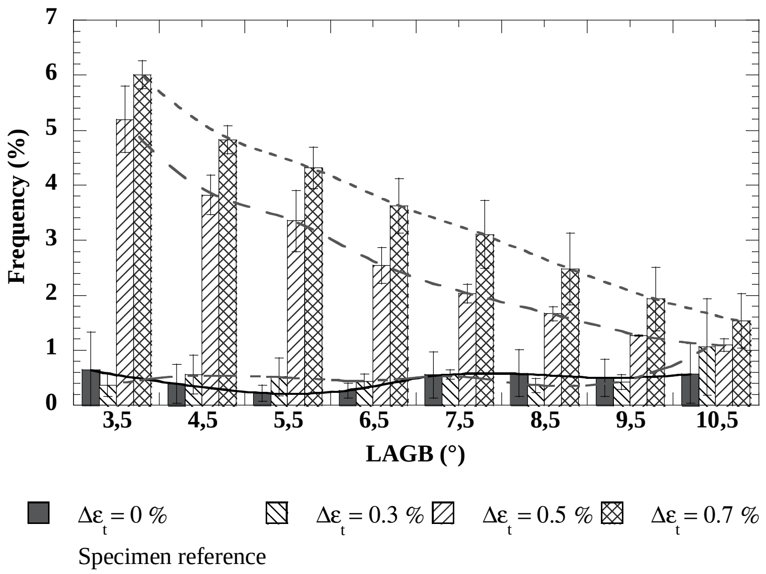

Figure 6 – Frequency distribution of LAGB (between 3° and 10°) before fatigue (reference specimen) and after fatigue at $\Delta\varepsilon_t$=0.3%, $\Delta\varepsilon_t$= 0.5% and $\Delta\varepsilon_t$=0.7%.

In this way, since a relationship appears between dislocations structures and LAGB, LAGB can be used as a damage criterion. This has to be completed by a local strain assessment criterion, such as Kernel Average Misorientation (KAM) parameter.

- KAM parameter

KAM characterises misorientations referring to local orientation gradients. The KAM is calculated by determining the average of all misorientation angles between a pixel and all his neighbour pixels. Misorientations larger than 5° are considered as grain boundaries (HAGB or LAGB). The KAM is considered to be a damage criterion [7], [8], [17], [18]. The local misorientation is calculated as followed:

$$\langle KAM\rangle = exp\left[\frac{1}{N}\sum_{pi=1}^{N} ln\{KAM(pi)\}\right] \quad (1)$$

$$KAM_{pi} = \frac{1}{4}\sum_{i=1}^{4}\Delta\theta_{\mathrm{i}},\ \Delta\theta_{\mathrm{i}} < \Delta\theta_{\mathrm{lim}} \quad (2)$$

The local misorientation map of the reference specimen ($\Delta\varepsilon_t$=0% - unfatigued), as well as, the deformed samples ($\Delta\varepsilon_t$=0.5% and $\Delta\varepsilon_t$=0.7%) are shown in Figure 7. Specimens can be divided into two groups. The first has a very low and uniform KAM repartition. It concerns unfatigued specimen, as well as the specimen fatigued at $\Delta\varepsilon_t$=0.3%. The unfatigued specimen gives the KAM reference for the material. For $\Delta\varepsilon_t$=0.3%, though the specimen was cycled until fracture, no local misorientation was induced. A slight recovery is even observable as show in Figure 8. $\Delta\varepsilon_t$=0.5% and 0.7% specimens show different behaviours. Due to large plastic strain, a high amount of local misorientation develops. The plastic strain in the $\Delta\varepsilon_t$=0.7% specimen is so high that local misorientation spreads out in all grains. For the $\Delta\varepsilon_t$=0.5% specimen, a lower strain loading associated to microstructural inhomogeneities lead to the development of a local misorientation in selected grains.

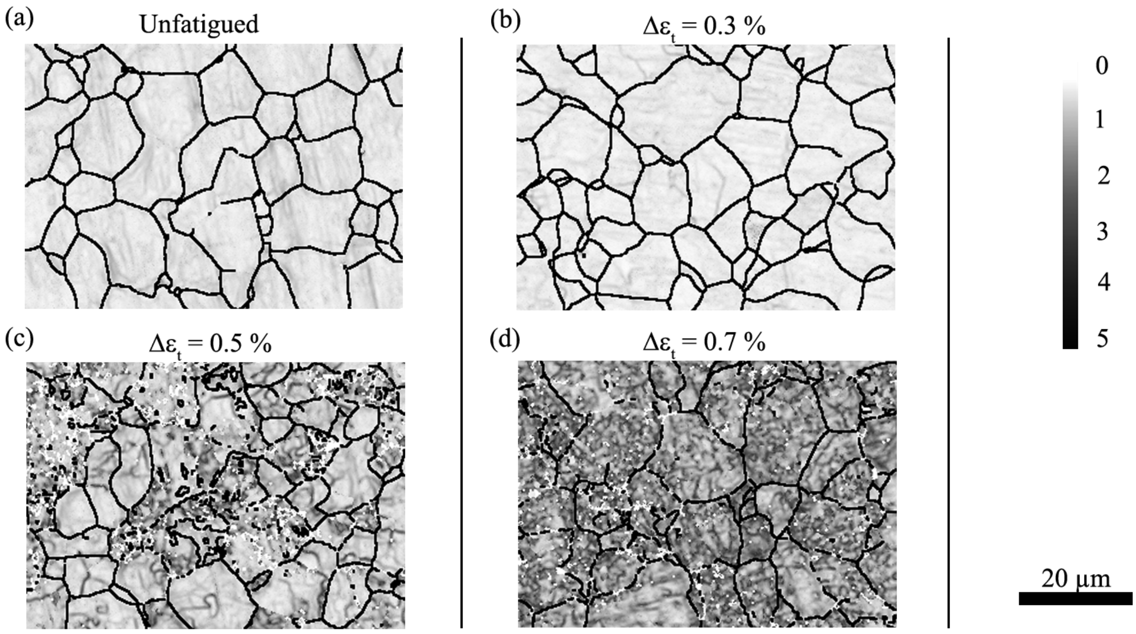

Figure 7 – Local misorientation map for the unfatigued specimen ($\Delta\varepsilon_t$=0%) (a), the $\Delta\varepsilon_t$=0.3% fatigued specimen (b), $\Delta\varepsilon_t$=0.5% fatigued specimen (c) and the $\Delta\varepsilon_t$=0.7% fatigued specimen (d).

Two microstructural criteria (LAGB and KAM) have been determined for lab tested material. A validation of those criteria for more complex structure (such as fan) is required for the comprehension of alternator fan damage.

6 DISCUSSION

A way to link macroscopic strain to KAM, that assesses the local cyclic plasticity in a quantitative manner is to study the relative change between unfatigued (reference) and deformed material [18]. The formula (equation (3)) has then be considered. The results are presented Figure 8.

$$\Delta KAM_j = \frac{\langle KAM_i \rangle - \langle KAM_j \rangle}{\langle KAM_j \rangle} \times 100 \quad (3)$$

where, i is the considered sample and j the reference sample.
When considering the alternator fan, a possible pre-strain resulting from the forming process may affect the KAM value. For this reason, each group of samples has his own reference sample, as defined in
Table 3.

Table 3 - EBSD specimens and their corresponding reference sample.

EBSD specimens	Corresponding reference specimen
Fatigue lab specimens ($\Delta\varepsilon_t$=0.3%, 0.5%, 0.7%)	Uncycled lab specimen
Unfatigued area of the unused fan	Uncycled lab specimen
Unfatigued area of the cycled fan	Uncycled lab specimen
Blade n°6 of an unused fan	Unfatigued area far from blade n°6 of the unused fan
Blade n°6 of an cycled fan	Unfatigued area far from blade n°6 of the cycled fan

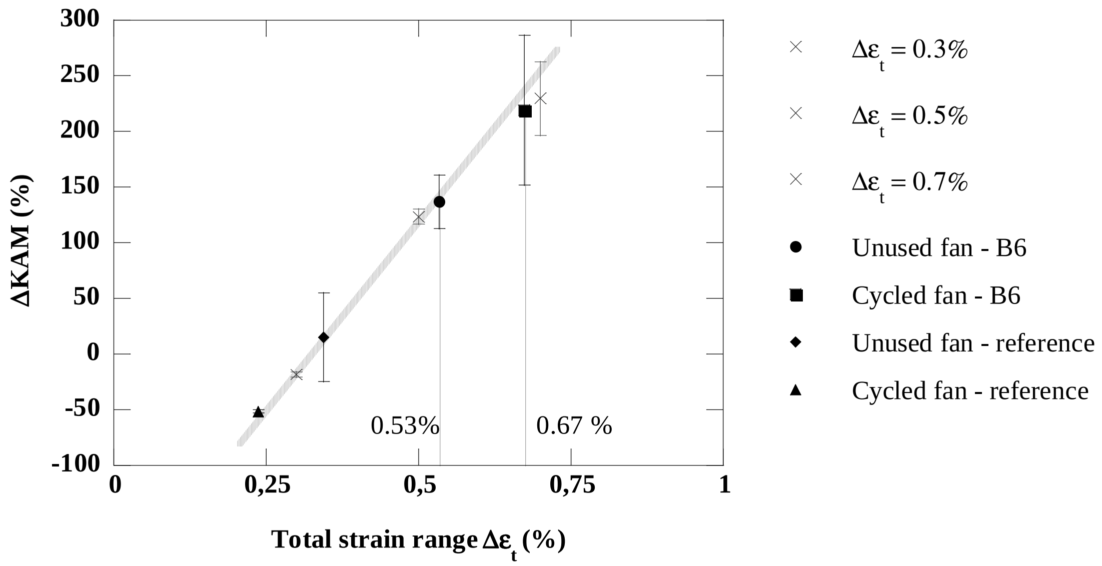

Figure 8 – Relative change in the local misorientation compared with KAM value reference.

The changes in term of local misorientation (expressed by ΔKAM as a function of the total strain range $\Delta\varepsilon_t$) are reported on the Figure 8. The dotted line represents the change in local misorientation of fatigue specimens, compared to local misorientation of an uncycled lab specimen. Some observations can be made:

- Considering the fatigue lab specimens, the evolution of ΔKAM as a function of $\Delta\varepsilon_t$ is rather linear. Furthermore, the more the macroscopic applied strain increases, the more the standard deviation increases. Besides, $\Delta\varepsilon_t$=0.3% specimen exhibits a negative ΔKAM value, which means that the local deformation is lower than in case of the unfatigued specimen. However, as mentioned previously, the unfatigued specimen is not free of dislocations. The low strain amplitude loading leads to a slight recovery. On the opposite, at higher strain levels, cyclic loading leads to generate dislocations, which arrange into dislocations cell structures and high local misorientation values.
- Regarding the fan references (unused and cycled fan), ΔKAM values are rather low, although these latter remain different. Indeed, the cycled reference fan has a negative ΔKAM. A hypothesis is that cyclic loading in service has led to a strain recovery too. These observations also point out a scattering of the results, due to the fact that all the studied specimens (lab specimens and fans) are industrial material. As a consequence, this should be integrated in the final life prediction model.
- The blade n°6 of the unused fan has a ΔKAM value of 133%. This can be related to the forming process that induces local deformation in this area.
- The blade n°6 of the cycled fan exhibits a very high ΔKAM value (219%). Here, a combination of forming process and fatigue phenomenon during service can lead to a high strained area.
- The study shows that the KAM method can consider deformation in a material but cannot take into account the nature of deformation, monotonic or loading.

A relationship between ΔKAM and the local cyclic strain for the lab specimens and representative of the material behaviour has been established. Then, taking into account the ΔKAM value of the cycled fan and simply referring to Figure 8, would suggest that the total strain in the blade n°6 is equivalent to a strain value of 0.67%.

Nevertheless, this should be put into perspective since the uncycled fan exhibits a ΔKAM value corresponding to a strain value of 0.53%, certainly inherent to the forming process.

7 CONCLUSION AND PERSPECTIVES

The fatigue behaviour of a ferritic steel has been studied and shows a dependence upon the applied strain range. For the highest strain tests TEM observations did not allow to distinguish the materials. This has been overcame through EBSD experiments, especially by employing the KAM method. The procedure has been applied to the material taken from an alternator fan.

8 ACKNOWLEDGMENTS

This work was supported by the Agence de l'Environnement et de la Maitrise de l'Energie (ADEME) through the Mhygale project.

9 REFERENCES

[1] F. A. Conle and C.-C. Chu, *Int. J. Fatigue*, 19, 1997, 317-323.
[2] M. Haiba, D. Barton, P. Brooks, and M. Levesley, *Comput. Struct.*, 80, 2002, 481-494.
[3] R. Schneider, U. Wuttke & C. Berger, *Procedia Eng. 2*, 2010, 2357-2366
[4] S. K. Koh, *Eng. Fail. Anal.*, 16, 2009, 914-922.
[5] J. Lim, S. Hong, and S. Lee, *Int. J. Fatigue*, 27, 2005, 1653-1660.
[6] J.-B. Vogt, S. Argillier, J.-P. Massoud, and V. Prunier, *Eng. Fail. Anal.*, 7, 2000, 301-310.
[7] S. Zaefferer, P. Romano, and F. Friedel, *J. Microscop.*, (230), 2008, 499-508.
[8] R. Petrov, L. Kestens, a Wasilkowska, and Y. Houbaert, *Mater. Sci. Eng. A*, 447, 2007, 285-297.
[9] R. H. Petrov, J. Bouquerel, K. Verbeken, L. A. I. Kestens, P. Verleysen, and Y. Houbaert, *Mater. Sci. Forum*, 2010, 3447-3452.
[10] M. Kamaya, *Mater. Charact.*, 60, 2009, 125-132.
[11] M. Kamaya, A. Wilkinson, and J. Titchmarsh, *Nucl. Eng. Des.*, 235, 2005, 713-725.
[12] M. Kamaya, A. Wilkinson, and J. Titchmarsh, *Acta Mater.*, 54, 2006, 539-548.
[13] M. Caul and V. Randle, *Mater. Charact.*, 38, 1997, 155-163.
[14] P. J. Buchanan, V. Randle, and P. E. J. Flewitt, *Scripta Mater.*, 37, 1997, 1511-1518.
[15] P. Wu, H. Jin, Y. Shi, and D. Lloyd, *Mater. Sci. Eng. A*, 423, 2006, 300-305.
[16] M. Kamaya, *Mater. Charact.*, 60, 2009, 1454-1462.
[17] M. Kamaya, *Ultramicroscopy*, 111, 2011, 1189-1199.
[18] J. Bouquerel, Modelling and Characterisation of Multiphase TRIP steel under static and dynamic loading, PhD Thesis, Gent University, 2008.
[19] V. Randle, *Mater. Charact.*, 60, 2009, 913-922.
[20] Electron Backscatter Diffraction in Materials Science, A Schwartz, M Kumar and B Adams, Kluwer/Plenum 2nd ed, New York, 2009, 247-264.
[21] C.-C. Shih, N.-J. Ho, and H.-L. Huang, *Mater. Sci. Eng. A*, 517, 2009, 235-238.